You might find this additional information useful...

Supplemental material for this article can be found at:
http://ajpcell.physiology.org/cgi/content/full/ajpcell.00168.2009/DC1

This article cites 47 articles, 22 of which you can access free at:
http://ajpcell.physiology.org/cgi/content/full/298/3/C477#BIBL

Updated information and services including high-resolution figures, can be found at:
http://ajpcell.physiology.org/cgi/content/full/298/3/C477

Additional material and information about *AJP - Cell Physiology* can be found at:
http://www.the-aps.org/publications/ajpcell

This information is current as of June 10, 2010 .

Iron supply determines apical/basolateral membrane distribution of intestinal iron transporters DMT1 and ferroportin 1

Marco T. Núñez,[1,2] **Victoria Tapia,**[1,2] **Alejandro Rojas,**[2] **Pabla Aguirre,**[2] **Francisco Gómez,**[1,2] **and Francisco Nualart**[3]

[1]*Department of Biology, Faculty of Sciences, Universidad de Chile, Santiago, Chile;* [2]*Cell Dynamics and Biotechnology Institute, Santiago, Chile;* [3]*Department of Cell Biology, Faculty of Biological Sciences, Santiago, Chile and Department of Cell Biology, Universidad de Concepción, Concepción, Chile*

Núñez MT, Tapia V, Rojas A, Aguirre P, Gómez F, Nualart F. Iron supply determines apical/basolateral membrane distribution of intestinal iron transporters DMT1 and ferroportin 1. *Am J Physiol Cell Physiol* 298: C477–C485, 2010. First published December 9, 2009; doi:10.1152/ajpcell.00168.2009.—Intestinal iron absorption comprises the coordinated activity of the influx transporter divalent metal transporter 1 (DMT1) and the efflux transporter ferroportin (FPN). In this work, we studied the movement of DMT1 and FPN between cellular compartments as a function of iron supply. In rat duodenum, iron gavage resulted in the relocation of DMT1 to basal domains and the internalization of basolateral FPN. Considerable FPN was also found in apical domains. In Caco-2 cells, the apical-to-basal movement of cyan fluorescent protein-tagged DMT1 was complete 90 min after the addition of iron. Steady-state membrane localization studies in Caco-2 cells revealed that iron status determined the apical/basolateral membrane distribution of DMT1 and FPN. In agreement with the membrane distribution of the transporters, ^{55}Fe flux experiments revealed inward and outward iron fluxes at both membrane domains. Antisense oligonucleotides targeted to DMT1 or FPN inhibited basolateral iron uptake and apical iron efflux, respectively, indicating the participation of DMT1 and FPN in these fluxes. The fluxes were regulated by the iron supply; increased iron reduced apical uptake and basal efflux and increased basal uptake and apical efflux. These findings suggest a novel mechanism of regulation of intestinal iron absorption based on inward and outward fluxes at both membrane domains, and repositioning of DMT1 and FPN between membrane and intracellular compartments as a function of iron supply. This mechanism should be complementary to those based in the transcriptional or translational regulation of iron transport proteins.

intestinal iron absorption; divalent metal transporter 1; mucosal block

IN THE ABSENCE OF A CONTROLLED excretion mechanism, iron levels in the body are regulated mainly by its passage through the duodenum epithelia. Traditionally, intestinal iron absorption is divided into three sequential steps: the uptake of iron from the intestinal lumen; an intracellular phase, in which iron binds to cytosolic components; and a transfer step, in which iron passes from the cells to the blood plasma. The uptake of iron from the lumen of the intestine is mediated by the Fe^{2+}-H^+ cotransporter divalent metal transporter 1 (DMT1) (19).

Once inside the enterocyte, iron integrates into a cytosolic pool of weakly bound iron called the labile iron pool (LIP) (16, 25). The nature of the LIP-binding counterpart is unknown, but it has been ascribed to diverse low-molecular-weight substances such as phosphate, nucleotides, hydroxyl, amino, and sulfhydryl groups (23, 36). From the LIP, iron distributes into ferritin and other iron-requiring proteins (15, 24). Iron exit from the enterocyte is mediated by the efflux transporter ferroportin (FPN), the only member of the SLC40 family of transporters and the first reported protein that mediates the exit of iron from cells (30).

Regulation of intestinal iron absorption on the basis of body stores is mediated by hepcidin, a small peptide whose secretion by the liver is regulated by anemia, hypoxia, and the level of circulating iron (33). Following hepcidin treatment of intestinal cell lines, DMT1 levels are reduced (10, 31), whereas it induces a temporary decrease of FPN protein in macrophages (12). Following a hemolytic stimulus, a 3-day delay was noted before a significant decrease in circulating hepcidin was observed, and a further 24 h were necessary to observe increased duodenal expression of DMT1, duodenal cytochrome *b* ferrireductase, and FPN (17). Thus, the adaptive response to an iron challenge mediated by hepcidin is slow. A faster adaptive response is known as the mucosal block. The mucosal block phenomenon describes the ability of an initial dose of ingested iron to block absorption of a second dose given 2–4 h later (35, 40, 41). Given the short period of time involved in the blocking process, a change in hepcidin gene expression cannot explain the mucosal block. The intestinal epithelium probably has a complementary form of regulation based on the iron content of the intestinal lumen or, more likely, the intestinal cells (3, 43). The mucosal block process has received scant attention despite its potential relevance as a mechanism to impede absorption of large amounts of iron from a large ingestion. Recent works have described two possible mechanisms that could be involved in the mucosal block. Three hours after oral administration of iron, reductions in mRNA and protein expression of both DMT1 and Dcytb were noted. These changes, associated with decreased activity of iron regulatory proteins, were reported as possible causes of the mucosal block phenomenon (18). In another report, it was observed that iron given to fasting rats induced internalization of DMT1 from the apical membrane to intracellular compartment(s), followed by a decrease in DMT1 protein 6 h after dietary iron supplementation (47). Thus, subtraction of DMT1 from the apical membrane may underlie the mucosal block phenomenon.

Classically, DMT1 is ascribed to the apical membrane, whereas FPN is located in the basolateral membrane (14, 38). Nevertheless, there is scant but convincing evidence that FPN (26, 44) and DMT1 (6) are located in both the apical and basolateral domains. In iron-starved rats and Caco-2 cells, DMT1 shows a marked brush border distribution, but iron feeding promotes a fast (10–400 min) internalization of DMT1

Address for reprint requests and other correspondence: M. T. Núñez, Departamento de Biología, Facultad de Ciencias, Universidad de Chile, Las Palmeras 3425, Santiago, Chile (e-mail: mnúñez@uchile.cl).

into the apical cytoplasm (28, 29). This redistribution was interpreted as evidence of a process in which vesicles containing DMT1-iron could fuse with and pass the iron to vesicles containing apo-transferrin (28, 29). Nevertheless, the possibility of a regulatory mechanism that involves the movement of transporters in response to iron was left open.

Under the hypothesis that iron fluxes in intestinal cells may be determined by the activity of import and export transporters at both the apical and basolateral membranes, we studied apical and basolateral localization of these transporters, the associated apical and basolateral iron fluxes, and their response to the iron status of the cells.

EXPERIMENTAL PROCEDURES

Cells. Human Caco-2 cells [HTB-37, American Type Culture Collection (ATCC), Rockville, MD] were cultured in Dulbecco's modified Eagle's medium (DMEM) supplemented with 10% fetal bovine serum (FBS, Invitrogen-Gibco Life Technologies). For biotinylation and ^{55}Fe transport studies, cells were grown for 14–16 days in 12-mm diameter bicameral inserts (Corning-Costar). Before the start of the experiments, transepithelial resistance (TER) was measured to assess the integrity of the cell monolayer, and inserts with TER below 250 $\Omega \cdot cm^2$ were discarded (3).

Antibodies. Anti-FPN is a mouse monoclonal antibody prepared by the Immunology Services Center, Faculty of Sciences, Universidad de Chile against the carboxyl-terminal sequence CGPDEKEVTKEN QPNTSVV, the consensus motif for rat, mouse, and human FPN. In the past, we successfully used this polypeptide sequence for the preparation of a rabbit polyclonal antibody (2). In Western blot assays, the antibody recognized a band of 67 KDa molecular mass that was blocked when the antibody was coincubated with the immunogenic peptide (Fig. 1*C*). Pan-DMT1 is a rabbit polyclonal antibody that recognizes the amino-terminal sequence MVLGPEQKMSDDS VSGDH, present in all isoforms of human DMT1 (1). Rabbit polyclonal anti-glucose transporter 3 (Glut3) antibody was obtained from Abcam.

Positioning and movement of transporters in response to iron in rat duodenum. The positioning of DMT1 and FPN in rat duodenal cells was also determined before and after iron gavage by a modification of a described method (18). In brief, Sprague-Dawley rats were given an intragastric dose of iron (20 mg FeSO$_4$ in 250 µl 0.01 N HCl) prepared immediately before feeding; the solution contained a 5 M excess of ascorbic acid. The rats were anesthetized with ether 2.5 h after dosing, and the duodenum was isolated and snap-frozen in OCT embedding compound (Tissue-Tek). Tissue was sectioned in a cryostat for immunofluorescence. Sections (20 µm) were fixed for 30 min in 4% paraformaldehyde for DMT1 antibody or in Bouin's solution (Sigma) for FPN antibody, thawed in PBS (DMT1 antibody) or 70% ethanol (FPN antibody), and stored at −80°C until required. The treatment of animals complied with the Animal Care and Use guidelines of the Ethics Committee of the Faculty of Sciences, Universidad de Chile, and experiments were approved by the Ethics Committee.

Immunofluorescence detection of DMT1 and FPN in duodenum and Caco-2 cells was performed as described previously (31). Primary antibodies were detected with Alexa 546 goat anti-rabbit (DMT1) or Alexa 488 goat anti-mouse (FPN) (Invitrogen, Molecular Probes) at 1:500 dilutions. Omission of primary antibody during development resulted in no detectable signals. The nucleus was stained with TOPRO-3 (Invitrogen, Molecular Probes). Immunostaining was observed and photographed using a Zeiss LSM Meta confocal laser scanning microscope (Carl Zeiss, Göttingen, Germany).

Membrane biotinylation and Western blot analysis. The plasma membrane localization of DMT1 and FPN was studied by selective biotinylation of the apical and basolateral membranes of Caco-2 human intestinal epithelial cells (HTB-37, ATCC) as described pre-
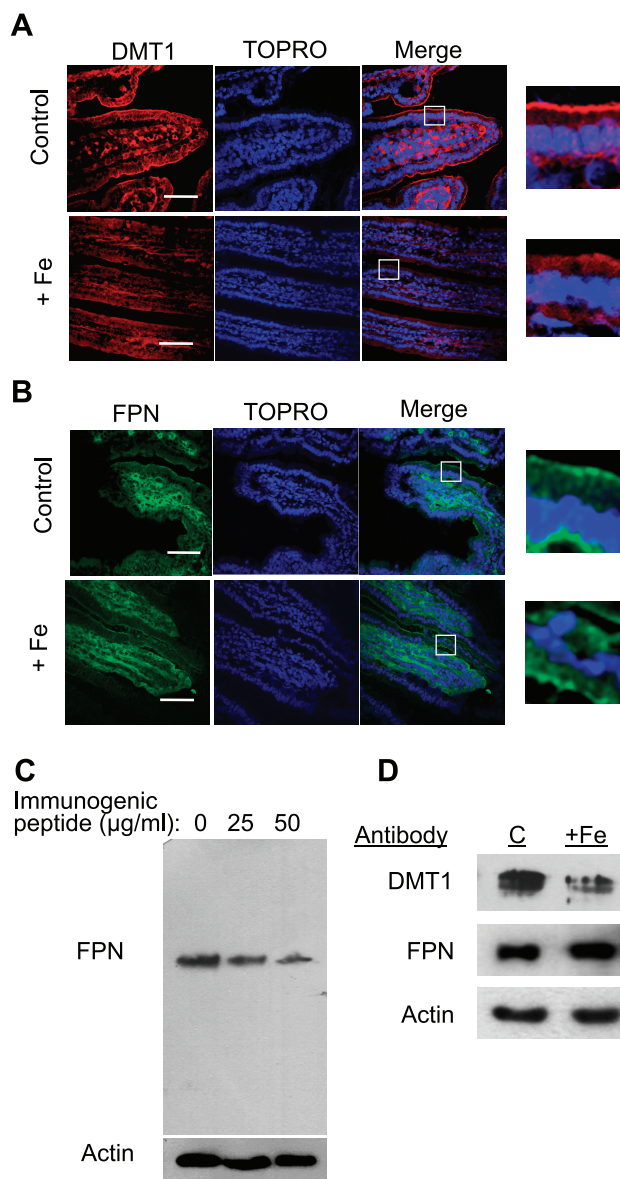
Fig. 1. Distribution of divalent metal transporter 1 (DMT1) and ferroportin (FPN) into apical and basolateral domains and the effect of iron supplementation. *A*: DMT1 localization (red) in the duodenum of fasting (control) and iron-stimulated (+Fe) rats 2.5 h after Fe gavage. Nuclear staining (blue, TOPRO) was included as a landmark. *B*: FPN localization (green) under fasting (control) and iron stimulation (+Fe) conditions as described above. Magnifications show FPN cell distribution under fasting (control) and iron stimulation (+Fe) conditions. Immunostaining without primary antibody gave no fluorescence signal (not shown). *A* and *B* scale bars, 60 µm. Similar results were obtained 3.5 h after gavage. The *right* panels in *A* and *B* show magnification of areas enclosed by the squares in the Merge frames. *C*: the monoclonal anti-FPN antibody used recognized a 67-KDa band in Western blot analysis. Specificity of the antibody was assessed by inhibition of its binding activity when 25 or 50 mg/ml of the peptide used as immunogen was added to the antibody mixture. *D*: Western blot analysis of Pan-DMT1 and FPN from duodenum brush border membranes prepared either from fasting rats [control (C)] or from rats 2.5 h after iron gavage. Iron gavage induced a decrease in DMT1 of 47.1 ± 6.8% ($P = 0.016$; $n = 3$) and an increase in FPN of 17.7 ± 0.57% ($P = 0.210$; $n = 4$) when compared with the fasting situation (means ± SE, $n = 3$).

viously (6, 48). Briefly, cells were incubated from the apical or the basolateral medium with 0.5 mg/ml *N*-hydroxysuccinimide-imino biotin (Pierce, Rockford, IL). Cellular extracts were prepared and precipitated with immobilized streptavidin (Pierce). The pellet was

dissolved in SDS loading buffer and resolved by 10% SDS-PAGE. The proteins were then transferred to a nitrocellulose membrane for Western blot analysis of DMT1 and FPN, which was carried out as described previously (2). The immunoreactive bands were developed with a peroxidase-based SuperSignal chemiluminescence assay kit (Pierce) and quantified with the Quantity One software (Bio-Rad).

To study the positioning of transporters in response to iron, Caco-2 cells grown in polycarbonate cell culture inserts (Transwell, Corning-Costar) were preconditioned overnight with low-iron medium [DMEM, 10% low-iron FBS (43)] and were then incubated for 4 h with varied concentrations of Fe offered as $FeCl_3$-sodium nitrilotri-acetate (Fe-NTA; 1:2.2 mol:mol), after which DMT1 and FPN distribution was determined by biotinylation and Western blot analysis.

Real-time movement of DMT1 was determined using confocal microscopy by following the movement of DMT1(+IRE) tagged with cyan fluorescent protein (DMT1-CFP) in the carboxyl terminal. To this end, 14-day insert-grown Caco-2 cells were transfected with the construct pcDNA3-DMT1(+IRE)-CFP as described previously (5). Two days after transfection, the cells were preconditioned by overnight incubation in low-iron medium. The cells were then challenged with 20 μM ferrous ammonium sulfate (*time 0*), and 1-μm optical cuts in the apical-basolateral axis were obtained every 1 min for a 90-min period.

^{55}Fe iron fluxes. The iron content of insert-grown Caco-2 cells was modified by culturing them for 2 days with complete medium to which Fe-NTA was added to reach iron concentrations ranging between 2 and 25 μM. For concentrations below 5 μM Fe, Chelex-treated low-iron serum was used (3). This iron loading protocol ensures homogenization of the intracellular ^{55}Fe/^{56}Fe pool (43). The addition of iron as the Fe-NTA complex assures the long-term solubility of iron in the culture medium.

For iron uptake determinations, insert-grown cells pretreated with varied concentrations of iron were challenged from either the apical or the basolateral medium with 5 μM ^{55}FeCl$_3$-ascorbate (1:20, mol:mol) dissolved in DMEM medium. In these experiments, Fe-ascorbate was preferred over Fe-NTA to avoid a possible interference of Dcytb ferrireductase on the uptake process. After incubation, the content of ^{55}Fe in the cells plus ^{55}Fe in the *trans*-medium was considered to be the total cell ^{55}Fe uptake. In iron efflux experiments, the cells were cultured for 2 days in media with different concentrations of iron using ^{55}Fe-NTA as a tracer. To estimate the specific activity of cellular ^{55}Fe, a sample of the culture medium was taken at the end of the incubation period for determination of both ^{55}Fe radioactivity and total iron content by atomic absorption spectrometry as described previously (32). ^{55}Fe efflux was determined at 37°C for varied times between 5 and 30 min. ^{55}Fe radioactivity in the apical or basolateral medium was then quantified and considered to be the effluxed iron. The efflux medium was DMEM with 100 μM diethylene triamine pentaacetic acid (DTPA). DTPA was necessary to avoid the recapture of effluxed iron (data not shown). To evaluate a potential interference of endogenous transferrin on basolateral iron uptake, cells were previously depleted of transferrin by two 30-min incubations in DMEM medium without serum.

Cell transfections with antisense oligonucleotides. Antisense MA1 oligonucleotide (4), here called ASDMT1, was used to effectively block DMT1 expression. Antisense sequences for FPN were selected to follow the strategy of Tu et al. (45), which disrupts splicing by targeting intronic or exonic sequences carrying the GGGA motif. From a total of six antisense sequences tested, the effect of ASFPN1 (GTGCCTCCCAGATGG, exon 2), ASFPN6 (GAGGGTCCCATGGCTC-CCACAC, intron 5) and ASFPN8 (TCCGTCCCACCCTGCC, intron 6) are reported here. The other three antisense sequences tested did not have a noticeable effect on FPN expression as determined by Western blot. For transfection, cells grown for 10 days in 0.33-cm^2 culture inserts were treated with 10 μg/ml antisense oligonucleotides in the presence of Lipofectamine following the instructions of the manufacturer (Gibco Life Sciences). ^{55}Fe uptake experiments were performed

3 days after transfection (4). DMT1 and FPN protein expression was evaluated by immunodetection as described previously (2).

Data analysis. All experiments were performed at least three times, and representative experiments are shown. One-way ANOVA was used to test differences in mean values, and Tukey's post hoc test was used for comparisons (In Stat, GraphPad Prism, San Diego, CA).

RESULTS

Effect of iron supplementation on apical/basolateral distribution of DMT1 and FPN. It is widely accepted that DMT1 transports iron from the intestinal lumen into the enterocyte, whereas FPN transports iron from the cell into the blood circulation. Nevertheless, recent evidence indicates the presence of FPN in the microvilli of the intestinal epithelium (44), an unlikely location considering the role of FPN as an iron efflux transporter. Similarly, overexpression of the hereditary hemochromatosis protein HFE induces redistribution of DMT1 to the basolateral membrane, a possible mechanism to down-regulate iron absorption (6). We expanded on these observations by studying the apical/basolateral location of DMT1 and FPN in rat duodenum in response to iron gavage. DMT1 and FPN localization was detected by immunofluorescence after 2.5 h of gavage (Fig. 1). DMT1 presented a marked apical distribution under control conditions, whereas iron induced a reduction of its membrane localization and an apparent decline in fluorescence intensity through the cytoplasm (Fig. 1*A*). In agreement with previous results (5, 44), FPN localized preferentially to the basolateral domain, but considerable FPN was also observed in the apical domain (Fig. 1*B*). Iron gavage induced a reduction of basolateral FPN without apparent effect on apical FPN (Fig. 1*B*). In concordance with previous findings (2), in Caco-2 cells the monoclonal anti-FPN antibody used in this study recognized a band of 67 KDa molecular mass in Western blot analysis. Coincubation of the antibody with the peptide used as immunogen markedly decreased the intensity of the 67-KDa band (Fig. 1*C*). We then determined DMT1 and FPN abundance in microvilli membrane obtained from fasting (control, C) and iron-fed rats. Iron feeding induced a drastic decrease of the DMT1+IRE isoform present in the microvilli membrane, whereas FPN increased nonsignificantly (Fig. 1*D*). Predictably, both apical membrane events, diminution of DMT1 and increase of FPN, should result in decreased apical iron uptake and, possibly, decreased iron transfer into the basolateral milieu.

Next, we characterized the kinetics of DMT1 relocalization by time-lapse confocal microscopy using polarized Caco-2 cells. Cells were transfected with a construct coding for DMT1-CFP, and its cellular localization after the addition of iron was determined from time-lapse apical-to-basal galleries (Fig. 2). Iron induced a time-dependent movement of DMT1 from apical into basal domains (Fig. 2*A*). The relocalization of DMT1 was relatively fast, being completed within 60–90 min (Fig. 2*B*). Taken together, the above experiments indicate that iron feeding results in the sequestration of DMT1 from the apical membrane and of FPN from the basolateral membrane. These movements should substantially decrease intestinal iron absorption, as described after gavage of iron-deficient rats (18).

Apical/basolateral membrane localization of DMT1 and FPN. The poor space resolution of conventional fluorescence microscopy makes it difficult to distinguish between localization to the membrane versus the peripheral cytosol. To ascer-
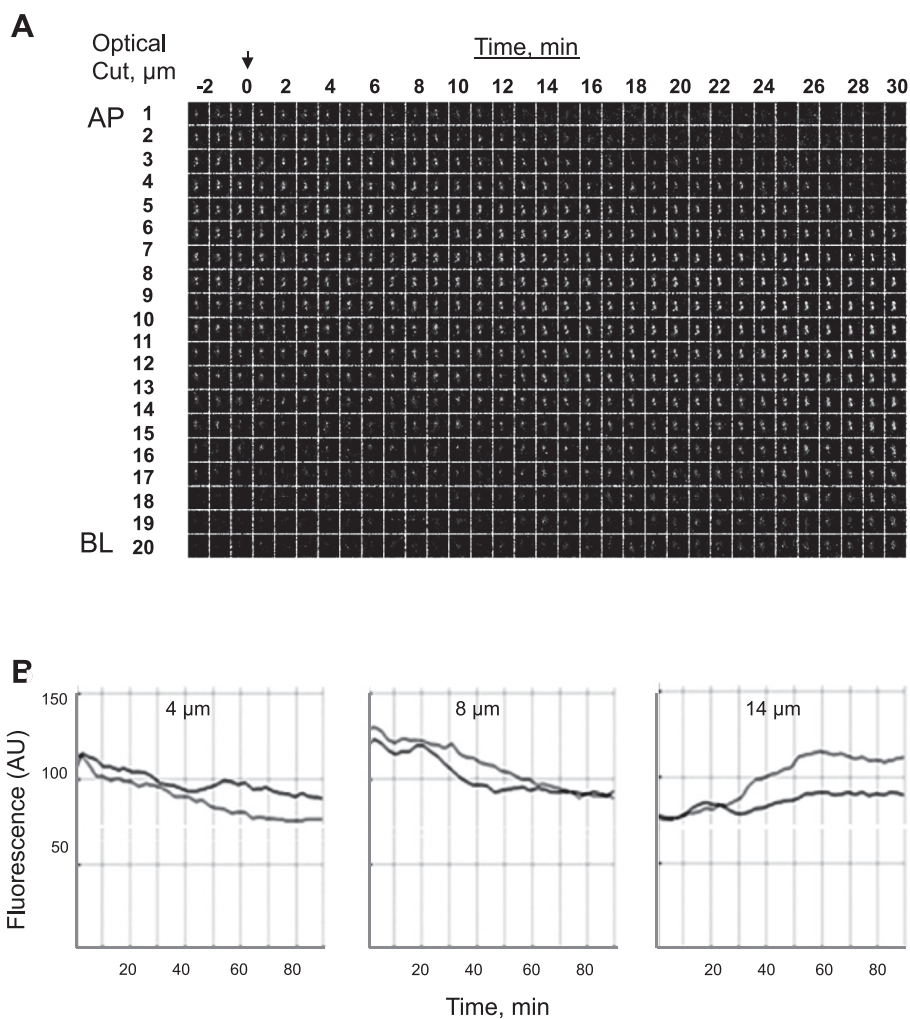
Fig. 2. Iron-induced apical-to-basal movement of DMT1 detected by fluorescence microscopy. *A*: Caco-2 cells expressing DMT1-cyan fluorescent protein (CFP) were challenged with 20 μM ferrous ammonium sulfate, and 20 apical-to-basal optical cuts of 1 μm were taken every 1 min before (−2 to 0 min) or after (0–30 min) the addition of iron (arrow). Changes in fluorescence are shown in the apical-basal axis of a group of two DMT1-CFP-expressing cells as a function of time. AP, apical; BL, basolateral. *B*: quantification of the changes in fluorescence of two DMT1-CFP-expressing cells (dark and light shaded lines) as a function of time (0–90 min), obtained at fixed distances of 4, 8, and 14 μm from the apical border. Shown is one of five similar experiments. AU, arbitrary units.

tain the membrane distribution of DMT1 and FPN, we selectively biotinylated the apical and basolateral membranes, an extremely sensitive method for studying membrane protein topology. Caco-2 cells grown in Transwell inserts showed a well-polarized phenotype, which was evident by the presence of Glut3 in the apical membrane (20) and of transferrin receptor 1 (TfR1) in the basolateral membrane (6) (Fig. 3*A*). The membrane distribution of the transporters was found to be a function of iron supply. Cells were preconditioned for 4 h with 2, 10, or 30 μM Fe in the culture medium and then tested for DMT1 and FPN membrane distribution (Fig. 3*B*). Quantification of band density indicated that the membrane distribution of DMT1 (Fig. 3*C*) changed as a function of iron supply. A significant reduction in apical membrane DMT1 ($P < 0.05$) was found between 2 μM Fe and both 10 and 30 μM Fe (Fig. 3*C*). Similarly, a significant increase in basolateral DMT1 ($P < 0.05$) was found between 2 and 30 μM Fe (Fig. 3*C*). Changes in FPN distribution were more subtle. An increase in apical FPN and a decrease in basolateral FPN, which that did not reach significance ($P = 0.062$ and $P = 0.066$, respectively), was apparent between 2 and 30 μM Fe (Fig. 3*D*). Thus, in Caco-2 cells, iron induced not only the relocalization of DMT1 to intracellular domains, but also induced its redistribution between the apical and basolateral membranes.

Apical and basolateral iron fluxes. To support a physiological function, the presence of DMT1 and FPN in the apical and basolateral membranes should be associated with corresponding inward and outward iron fluxes. To test for orthodox (apical uptake, basolateral efflux) and unorthodox (basolateral uptake, apical efflux) fluxes, iron uptake activity was determined in Caco-2 cells grown in bicameral inserts and challenged with ^{55}Fe from either the apical or the basolateral chamber. Similarly, iron efflux into the apical or basal chamber was determined in cells previously loaded with the isotope (Fig. 4). Besides the acknowledged apical-to-cell (Fig. 4*A*) and cell-to-basolateral (Fig. 4*D*) iron fluxes, Caco-2 cells also showed basolateral-to-cell (Fig. 4*B*) and cell-to-apical (Fig. 4*C*) iron fluxes. Part of the observed basolateral ^{55}Fe uptake could be due to endocytic uptake mediated by endogenous transferrin. This possibility was evaluated by depleting the cells of transferrin before the determination of ^{55}Fe uptake. Transferrin depletion produced a consistent 1.4-fold increase in basolateral uptake (Fig. 4*B*, open circle). This increase could be due to a priming of the basal uptake system by the procedure used to deplete endogenous transferrin. The sum of these results points to the presence of functional iron transporters at both the apical and the basolateral membranes.
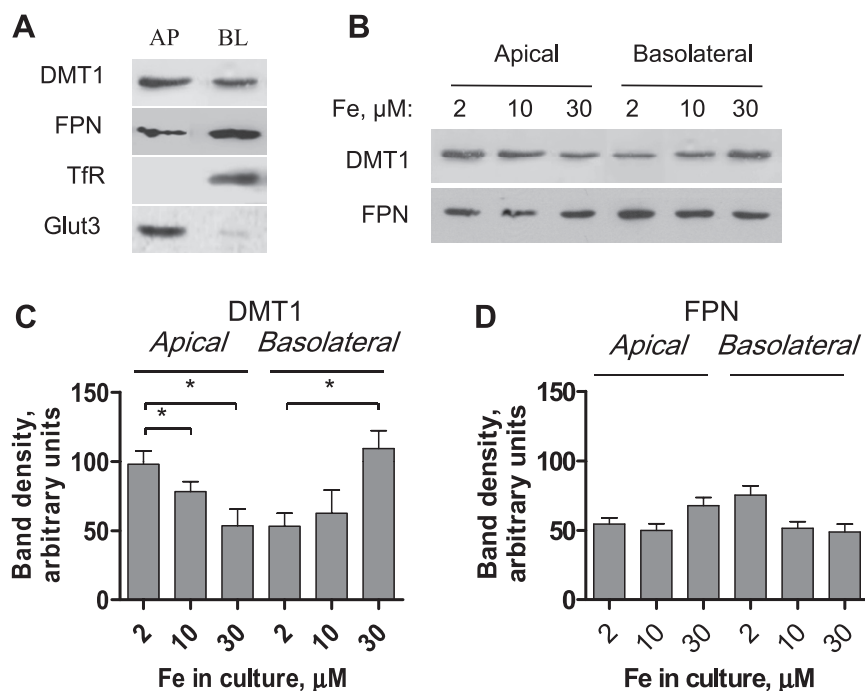
Fig. 3. Iron induces membrane relocalization of DMT1 and FPN. Caco-2 cells grown in bicameral inserts were biotinylated from the apical or basolateral medium. Biotin-containing proteins were selected by streptavidin-agarose binding, resolved by SDS-PAGE, and recognized with specific antibodies by Western blotting. *A*: membrane distribution of DMT1, FPN, glucose transporter 3 (Glut3; apical membrane marker), and transferrin receptor 1 (TfR1; basolateral membrane marker) under standard culture conditions (5 μM Fe). *B*: insert-grown cells were incubated for 4 h with varied iron concentrations before determination of DMT1 and FPN membrane distribution by biotinylation. A representative experiment is shown. *C* and *D*: densitometric analysis of the apical and basolateral distribution of DMT1 (*C*) and FPN (*D*) as a function of iron concentration. Values are means ± SE (n = 6). *$P < 0.05$.

Effect of DMT1 and FPN antisense oligonucleotides on iron fluxes. To determine the participation of DMT1 and FPN in the iron fluxes reported above, we knocked down DMT1 and FPN by antisense methodology and determined the resulting iron fluxes (Fig. 5). Treatment with antisense ASDMT1, ASFPN6, and ASFPN8 oligonucleotides decreased the expression of DMT1 with ASDMT1 or FPN with ASFPN6 and ASFPN8, whereas ASFPN1 had no effect on FPN expression (Fig. 5*A*). In addition, apical (Fig. 5*B*) and basolateral (Fig. 5*C*) iron uptake were effectively inhibited by ASDMT1 ($P < 0.05$), indicating the participation of DMT1 in both apical and basolateral iron uptake. ASFPN1 oligonucleotide produced no changes in apical or basolateral iron uptake, whereas ASFPN6 and ASFPN8 oligonucleotides induced an apparent increase in apical and basolateral iron uptake (Fig. 5, *B* and *C*), a rather unexpected finding. These increases could be due to an increase in DMT1 expression secondary to a decrease in FPN expression, but this possibility is not supported by Western blot analysis (Fig. 5*A*). Most probably, the increased uptake observed with FPN antisense DNAs is due to increased retention of iron by the cells due to decreased iron efflux. As expected, ASDMT1, ASFPN6, and ASFPN8 inhibited both apical-to-basolateral (Fig. 5*D*) and basolateral-to-apical (Fig. 5*E*) trans-epithelial iron transport, whereas ASFPN1 did not have a significant effect. Inhibition of trans-epithelial iron transport by ASDMT1 treatment is explained by decreased uptake at the apical or the basolateral membrane, whereas decreased trans-epithelial transport generated by ASFPN6 and ASFPN8 is explained by decreased exit of ^{55}Fe at both the apical and basolateral membranes. Together, the data strongly suggest that DMT1 and FPN are involved in the apical and the basolateral iron fluxes described here.
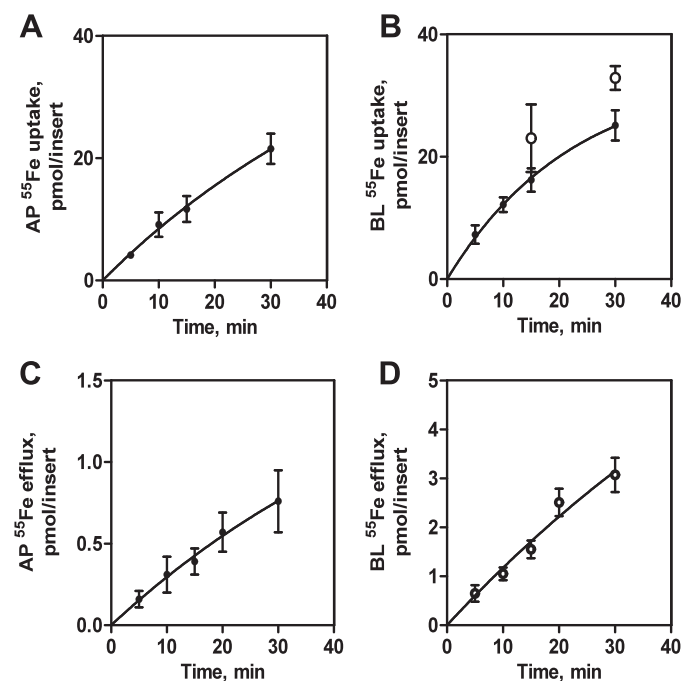
Dependence of iron fluxes on Fe concentration. Next, we examined whether preconditioning cells with various extracellular iron concentrations affected apical or basolateral fluxes (Fig. 6). As predicted by the membrane distribution of the transporters (Fig. 3), increasing extracellular iron resulted in a robust decrease in the apical uptake rate (Fig. 6*A*) and a decrease in the rate of transfer to the basolateral medium (Fig.

Fig. 4. Iron fluxes in Caco-2 cells. *A* and *B*: apical and basolateral iron uptake. Insert-grown cells were tested with 5 μM ^{55}Fe-ascorbate placed in the apical (*A*) or basolateral (*B*) medium. Empty circles in *B* correspond to basolateral iron uptake by cells previously depleted of transferrin. *C* and *D*: apical and basolateral iron efflux. Insert-grown cells were incubated for 24 h in regular medium supplemented with 1 μM ^{55}Fe-ascorbate. Cells were thoroughly washed, and ^{55}Fe efflux into the apical (*C*) or basolateral (*D*) medium was determined. Values are means ± SE of three experiments.
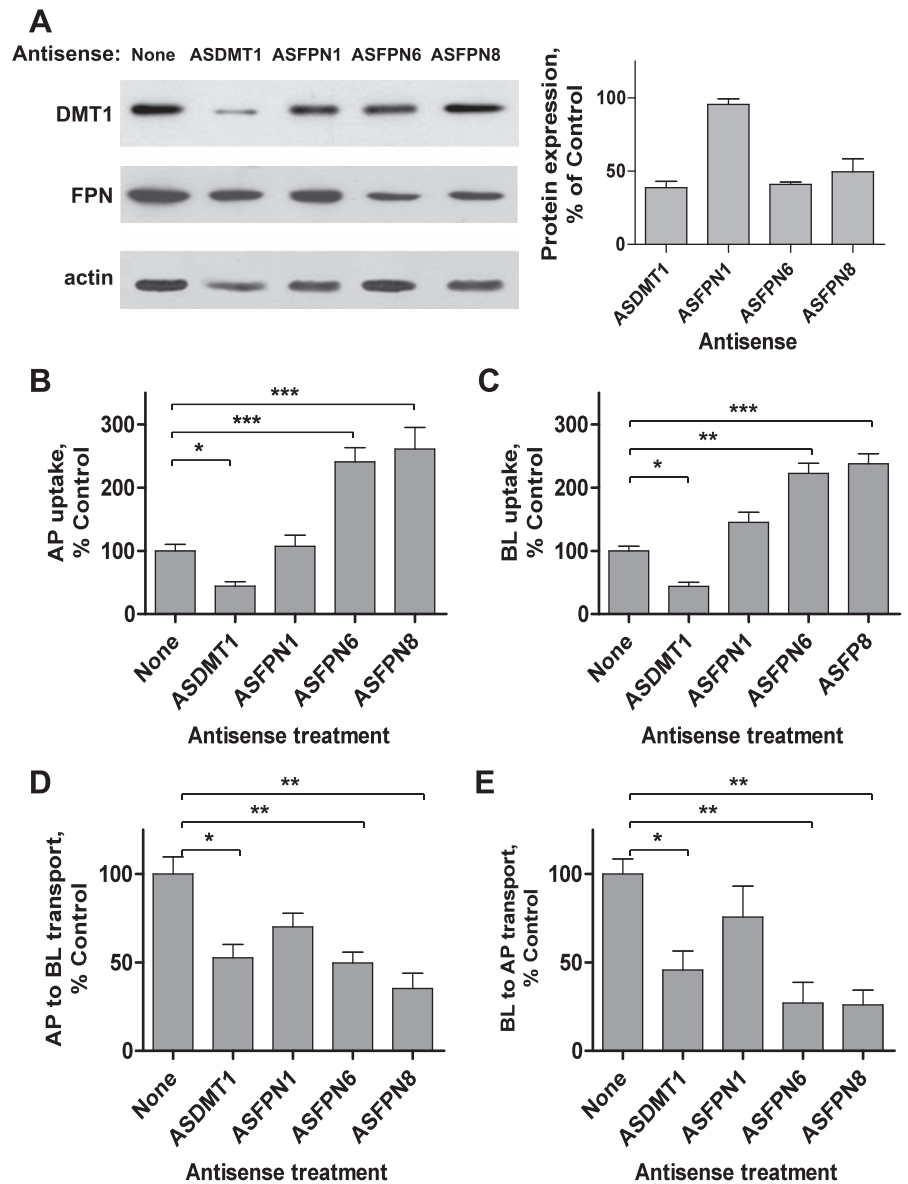
Fig. 5. Effect of DMT1 and FPN antisense oligonucleotides on iron fluxes. Insert-grown Caco-2 cells were treated for 48 h with antisense oligonucleotides against DMT1 (ASDMT1) or FPN (ASFPN1, ASFPN6, and ASFPN8) and then incubated from the apical or basolateral medium with $^{55}Fe^{2+}$-ascorbate (1:20, mol:mol) for 60 min as described in EXPERIMENTAL PROCEDURES. *A*: DMT1 and FPN protein expression determined by Western blot analysis after treatment with DMT1 or FPN antisenses. *Right*: means ± SE ($n = 3$) of band intensity normalized to control without treatment. *B–E*: antisense-treated cells were tested for apical (*B*) or basolateral (*C*) ^{55}Fe uptake, as well as apical-to-basolateral (*D*) or basolateral-to-apical (*E*) ^{55}Fe fluxes. ASFPN1, which did not have an effect on FPN expression, was included in this study as a negative control. Values are means ± SE of three independent experiments. *$P < 0.05$; **$P < 0.01$; ***$P < 0.001$.

6*D*), suggesting a regulatory process to avoid excessive absorption under iron-replete conditions. Interestingly, we found considerable iron uptake from the basolateral medium (Fig. 6*B*), but this uptake responded only marginally to the iron supplied in the preconditioning step. This activity increased 1.3-fold between 5 and 25 μM Fe, compared with a decrease of 1.9-fold in the apical uptake rate.

We also found substantial apical efflux activity that responded keenly to the iron concentration in the preconditioning step (Fig. 6*C*). With increasing iron, the apical iron efflux rate increased 8.6 times, accompanied by a 4.3-fold decrease in the basolateral efflux rate (Fig. 6*D*). The increase in apical efflux could be explained by the compounded effects of increased FPN and decreased DMT1 in this membrane domain.

The combined results of these experiments indicate the presence of a robust system for the regulation of iron absorption by Caco-2 cells; an increase in iron supply not only decreases apical uptake and basolateral efflux, but also increases apical efflux. The significance of the basolateral uptake

activity described here is not clear, because free iron is not often found in the basolateral medium. Nevertheless, FPN-based basolateral activity could effect the recapture of freshly DMT1-effluxed iron.

DISCUSSION

Movement of transporters between the plasma membrane and intracellular domains is an important mechanism to regulate influx of ions and metabolites. Examples of this process are found in the transient receptor potential family of ion channels (8), the Glut4 transporter (13), neurotransmitter receptors (39), and aquaporin channels (34). Perhaps the most paradigmatic example of positional regulation is that of Glut4. In the basal state, Glut4 undergoes a slow cycling between the plasma membrane and intracellular compartments, with only a minor (5%) fraction of the total Glut4 protein pool localized to the plasma membrane. However, in response to insulin stimulation the rate of Glut4 exocytosis markedly increases so that
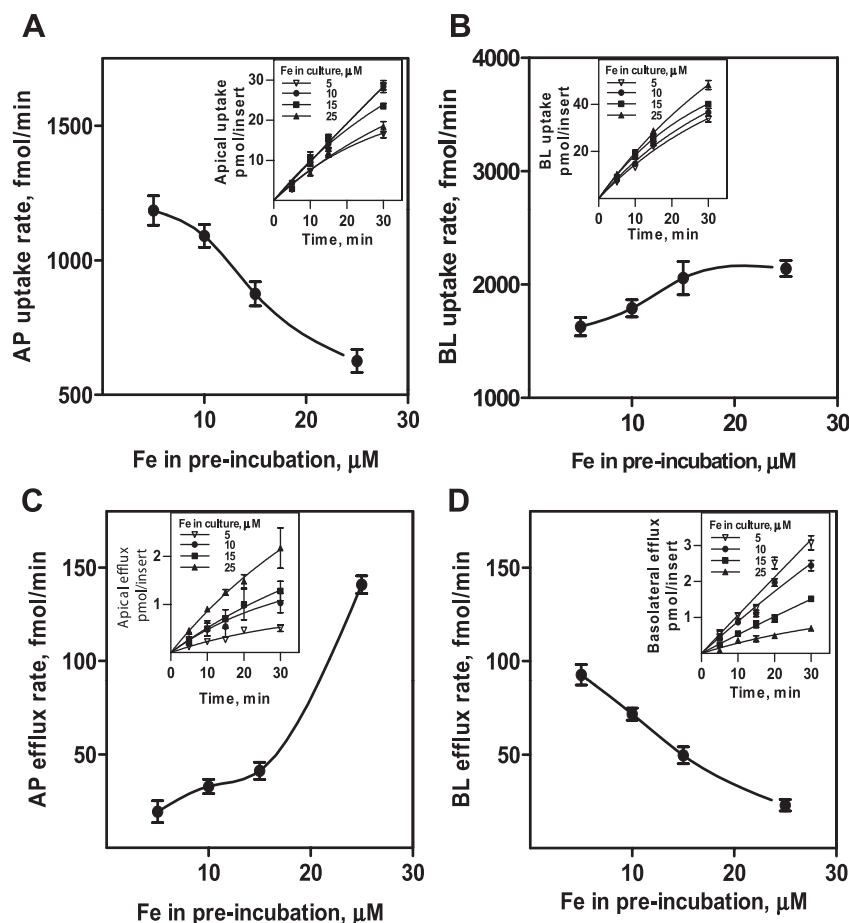
Fig. 6. Dependence of iron fluxes on iron concentration. *A* and *B*: insert-grown cells were preconditioned for 24 h with culture medium containing 5, 10, 15, or 25 μM FeCl₃-sodium nitrilotriacetate (Fe-NTA) and were then tested at different times for apical (*A*) and basolateral (*B*) ^{55}Fe uptake. *C* and *D*: similarly, cells were preequilibrated for 24 h in culture medium containing 5, 10, 15, or 25 μM ^{55}Fe before determination of ^{55}Fe efflux from either the apical (*C*) or the basolateral (*D*) membranes. Graphs show initial rates of uptake or efflux of ^{55}Fe as a function of the iron concentration in the preconditioning step. Initial rates were obtained from the corresponding kinetic curves shown in the *insets*. Values are means ± SE of three independent experiments.

~50% of the Glut4 proteins are relocated to the cell surface (21). Thus, the insertion or sequestration of a protein from the plasma membrane provides a fast and effective mechanism to regulate its function. In the frame of the experiments reported here, an increased iron offer seems to be a signal for a coordinated movement of DMT1 and FPN destined to decrease intestinal iron absorption.

We characterized the translocation of DMT1 and FPN between apical and basolateral domains as a function of iron supply in both rat duodenal intestine and polarized Caco-2 cells. Our findings reveal a novel mechanism by which intestinal cells regulate intestinal iron absorption through the repositioning of DMT1 and FPN in apical and basolateral membranes.

Besides its acknowledged location in the apical membrane, we found DMT1 in the basolateral membrane of Caco-2 cells and in basal domains of duodenal enterocytes. In retrospective, the finding of DMT1 in the basolateral membrane of Caco-2 cells or in the basal domains of enterocytes is not surprising, since DMT1 is needed for iron transport out of the endocytic vesicle during basolateral transferrin endocytosis (42).

Immunodetection evidenced FPN both at the apical and at the basal membrane, as well as strong staining of the cells in the lamina propria. At the basolateral membrane, FPN should be carrying its ascribed role of iron export transporter (30), but the presence of FPN in the apical membrane is intriguing. The presence of FPN in apical domains of absorbing enterocytes had been noticed previously (11, 44) although no functional role was ascribed to it. The results of this work support a putative role for apical FPN in a retrograde basal-to-apical iron flux in which non-transferrin-bound iron in the blood plasma is transported to the intestinal lumen.

The detection of FPN in cells of the lamina propria is interesting. It is possible that FPN fulfills a role in the passage of enterocyte-released iron into the blood circulation, since patients with ferroportin disease show a large iron accumulation in the cells of the lamina propria (9). Immunodetection of FPN in unfixed tissue also displayed labeling in the lamina propia, so it is improbable that labeling in this area was due to a fixation artifact (supplemental Fig. 1; supplemental data for this article can be found online at the *American Journal of Physiology-Cell Physiology* website).

Importantly, in Caco-2 cells, basolateral DMT1 and apical FPN emplacements were associated with concurrent iron fluxes, i.e., iron exit through the apical membrane and iron uptake from the basolateral milieu. Moreover, these fluxes were inhibited by antisense targeting of DMT1 or FPN, indicating that the fluxes were mediated, at least in part, by these transporters. The simplest interpretation of these findings is that Caco-2 cells have bidirectional iron fluxes at both the apical and basolateral membranes mediated by DMT1 and FPN.

We found that the relative abundance of DMT1 in the apical and basolateral membranes was a function of the iron content of the cells. Thus, under low-iron conditions, DMT1 was predominantly located in the apical membrane, whereas high-

iron conditions effected its repositioning to basal intracellular domains and the basolateral membrane. In agreement with other investigations (22, 47), we propose that the rapid withdrawal of DMT1 from the apical membrane accounts for the mucosal block phenomenon. Repositioning of DMT1 to basolateral domains was complete within 60–90 min after an iron challenge, a period similar to that reported for the mucosal block effect. A repositioning of DMT1 to the basolateral membrane is highly suggestive of a physiological response, because it could recapture iron exo-transported by FPN thus decreasing effective iron absorption.

Because rat duodenal epithelium also showed the presence of DMT1 and FPN in microvilli membranes, it is possible that the duodenal epithelium also has the potential for bidirectional fluxes at the apical and basolateral membranes. In this case, iron absorption from the intestinal lumen would be the result of a predominant iron inflow at the apical membrane and a predominant iron efflux at the basolateral membrane.

A considerable basolateral iron uptake activity was observed, which responded only marginally to the iron status of the cells. It is possible that, besides DMT1, an unidentified transport system not sensitive to iron status is contributing to basolateral iron uptake. Basolateral iron uptake is not expected to have a physiological function, since such an uptake needs non-transferrin-bound iron. Nevertheless, blood-to-lumen iron translocation could happen in the case of diseases where iron-binding capacity of transferrin is surpassed, such as β-thalassemia, hemoglobin E disease, and genetic hemochromatosis, in addition to the clinical condition of transfusional hemosiderosis (7, 27, 37). Under these conditions, plasma non-transferrin-bound iron, which can reach the micromolar range (7, 37, 46), could be safely transported to the intestinal lumen.

In summary, we found that DMT1 and FPN distribute to the apical and basolateral membranes of intestinal and Caco-2 cells as a function of the iron supply and iron status. The apical/basolateral positioning of DMT1 and FPN could be part of a fast physiological mechanism to avoid excessive iron absorption. It is possible that this movement is part of the mucosal block phenomenon, which precedes regulatory mechanisms of iron absorption based on gene expression. The discovery of a basolateral-to-apical transport process predicts a yet to be demonstrated system for the elimination of circulating non-transferrin-bound iron.

DISCLOSURES

No conflicts of interest are declared by the author(s).

REFERENCES

1. **Abouhamed M, Gburek J, Liu W, Torchalski B, Wilhelm A, Wolff NA, Christensen EI, Thevenod F, Smith CP.** Divalent metal transporter 1 in the kidney proximal tubule is expressed in late endosomal/lysosomal membranes: implications for renal handling of protein-metal complexes. *Am J Physiol Renal Physiol* 290: F1525–F1533, 2006.
2. **Aguirre P, Mena N, Tapia V, Arredondo M, Núñez MT.** Iron homeostasis in neuronal cells: a role for IREG1. *BMC Neurosci* 6: 3, 2005.
3. **Alvarez-Hernandez X, Nichols GM, Glass J.** Caco-2 cell line: a system for studying intestinal iron transport across epithelial cell monolayers. *Biochim Biophys Acta* 1070: 205–208, 1991.
4. **Arredondo M, Munoz P, Mura CV, Núñez MT.** DMT1, a physiologically relevant apical Cu^{1+} transporter of intestinal cells. *Am J Physiol Cell Physiol* 284: C1525–C1530, 2003.
5. **Arredondo M, Munoz P, Mura CV, Núñez MT.** HFE inhibits apical iron uptake by intestinal epithelial (Caco-2) cells. *FASEB J* 15: 1276–1278, 2001.
6. **Arredondo M, Tapia V, Rojas A, Aguirre P, Reyes F, Marzolo MP, Núñez MT.** Apical distribution of HFE-beta2-microglobulin is associated with inhibition of apical iron uptake in intestinal epithelia cells. *Biometals* 19: 379–388, 2006.
7. **Cabantchik ZI, Breuer W, Zanninelli G, Cianciulli P.** LPI-labile plasma iron in iron overload. *Best Pract Res Clin Haematol* 18: 277–287, 2005.
8. **Cayouette S, Boulay G.** Intracellular trafficking of TRP channels. *Cell Calcium* 42: 225–232, 2007.
9. **Corradini E, Montosi G, Ferrara F, Caleffi A, Pignatti E, Barelli S, Garuti C, Pietrangelo A.** Lack of enterocyte iron accumulation in the ferroportin disease. *Blood Cells Mol Dis* 35: 315–318, 2005.
10. **Chaston T, Chung B, Mascarenhas M, Marks J, Patel B, Srai SK, Sharp P.** Evidence for differential effects of hepcidin in macrophages and intestinal epithelial cells. *Gut* 57: 374–382, 2008.
11. **Chung B, Chaston T, Marks J, Srai SK, Sharp PA.** Hepcidin decreases iron transporter expression in vivo in mouse duodenum and spleen and in vitro in THP-1 macrophages and intestinal Caco-2 cells. *J Nutr* 139: 1457–1462, 2009.
12. **Delaby C, Pilard N, Goncalves AS, Beaumont C, Canonne-Hergaux F.** Presence of the iron exporter ferroportin at the plasma membrane of macrophages is enhanced by iron loading and down-regulated by hepcidin. *Blood* 106: 3979–3984, 2005.
13. **Dugani CB, Klip A.** Glucose transporter 4: cycling, compartments and controversies. *EMBO Rep* 6: 1137–1142, 2005.
14. **Dunn LL, Rahmanto YS, Richardson DR.** Iron uptake and metabolism in the new millennium. *Trends Cell Biol* 17: 93–100, 2007.
15. **El-Shobaki FA, Rummel W.** Mucosal transferrin and ferritin factors in the regulation of iron absorption. *Res Exp Med (Berl)* 171: 243–253, 1977.
16. **Epsztejn S, Kakhlon O, Glickstein H, Breuer W, Cabantchik I.** Fluorescence analysis of the labile iron pool of mammalian cells. *Anal Biochem* 248: 31–40, 1997.
17. **Frazer DM, Inglis HR, Wilkins SJ, Millard KN, Steele TM, McLaren GD, McKie AT, Vulpe CD, Anderson GJ.** Delayed hepcidin response explains the lag period in iron absorption following a stimulus to increase erythropoiesis. *Gut* 53: 1509–1515, 2004.
18. **Frazer DM, Wilkins SJ, Becker EM, Murphy TL, Vulpe CD, McKie AT, Anderson GJ.** A rapid decrease in the expression of DMT1 and Dcytb but not Ireg1 or hephaestin explains the mucosal block phenomenon of iron absorption. *Gut* 52: 340–346, 2003.
19. **Gunshin H, Mackenzie B, Berger UV, Gunshin Y, Romero MF, Boron WF, Nussberger S, Gollan JL, Hediger MA.** Cloning and characterization of a mammalian proton-coupled metal-ion transporter. *Nature* 388: 482–488, 1997.
20. **Harris DS, Slot JW, Geuze HJ, James DE.** Polarized distribution of glucose transporter isoforms in Caco-2 cells. *Proc Natl Acad Sci USA* 89: 7556–7560, 1992.
21. **Hou JC, Pessin JE.** Ins (endocytosis) and outs (exocytosis) of GLUT4 trafficking. *Curr Opin Cell Biol* 19: 466–473, 2007.
22. **Johnson DM, Yamaji S, Tennant J, Srai SK, Sharp PA.** Regulation of divalent metal transporter expression in human intestinal epithelial cells following exposure to non-haem iron. *FEBS Lett* 579: 1923–1929, 2005.
23. **Kakhlon O, Cabantchik ZI.** The labile iron pool: characterization, measurement, and participation in cellular processes(1). *Free Radic Biol Med* 33: 1037–1046, 2002.
24. **Kolachala VL, Sesikeran B, Nair KM.** Evidence for a sequential transfer of iron amongst ferritin, transferrin and transferrin receptor during duodenal absorption of iron in rat and human. *World J Gastroenterol* 13: 1042–1052, 2007.
25. **Kruszewski M.** The role of labile iron pool in cardiovascular diseases. *Acta Biochem Pol* 51: 471–480, 2004.

26. **Laftah AH, Sharma N, Brookes MJ, McKie AT, Simpson RJ, Iqbal TH, Tselepis C.** Tumour necrosis factor alpha causes hypoferraemia and reduced intestinal iron absorption in mice. *Biochem J* 397: 61–67, 2006.

27. **Le Lan C, Loreal O, Cohen T, Ropert M, Glickstein H, Laine F, Pouchard M, Deugnier Y, Le Treut A, Breuer W, Cabantchik ZI, Brissot P.** Redox active plasma iron in C282Y/C282Y hemochromatosis. *Blood* 105: 4527–4531, 2005.

28. **Ma Y, Specian RD, Yeh KY, Yeh M, Rodriguez-Paris J, Glass J.** The transcytosis of divalent metal transporter 1 and apo-transferrin during iron uptake in intestinal epithelium. *Am J Physiol Gastrointest Liver Physiol* 283: G965–G974, 2002.

29. **Ma Y, Yeh M, Yeh KY, Glass J.** Iron Imports. V. Transport of iron through the intestinal epithelium. *Am J Physiol Gastrointest Liver Physiol* 290: G417–G422, 2006.

30. **McKie AT, Marciani P, Rolfs A, Brennan K, Wehr K, Barrow D, Miret S, Bomford A, Peters TJ, Farzaneh F, Hediger MA, Hentze MW, Simpson RJ.** A novel duodenal iron-regulated transporter, IREG1, implicated in the basolateral transfer of iron to the circulation. *Mol Cell* 5: 299–309, 2000.

31. **Mena NP, Esparza A, Tapia V, Valdes P, Núñez MT.** Hepcidin inhibits apical iron uptake in intestinal cells. *Am J Physiol Gastrointest Liver Physiol* 294: G192–G198, 2008.

32. **Mura CV, Delgado R, Aguirre P, Bacigalupo J, Núñez MT.** Quiescence induced by iron challenge protects neuroblastoma cells from oxidative stress. *J Neurochem* 98: 11–19, 2006.

33. **Nicolas G, Chauvet C, Viatte L, Danan JL, Bigard X, Devaux I, Beaumont C, Kahn A, Vaulont S.** The gene encoding the iron regulatory peptide hepcidin is regulated by anemia, hypoxia, and inflammation. *J Clin Invest* 110: 1037–1044, 2002.

34. **Noda Y, Sasaki S.** Regulation of aquaporin-2 trafficking and its binding protein complex. *Biochim Biophys Acta* 1758: 1117–1125, 2006.

35. **O'Neil-Cutting MA, Crosby WH.** Blocking of iron absorption by a preliminary oral dose of iron. *Arch Intern Med* 147: 489–491, 1987.

36. **Petrat F, de Groot H, Sustmann R, Rauen U.** The chelatable iron pool in living cells: a methodically defined quantity. *Biol Chem* 383: 489–502, 2002.

37. **Pootrakul P, Breuer W, Sametband M, Sirankapracha P, Hershko C, Cabantchik ZI.** Labile plasma iron (LPI) as an indicator of chelatable plasma redox activity in iron-overloaded beta-thalassemia/HbE patients treated with an oral chelator. *Blood* 104: 1504–1510, 2004.

38. **Sharp P, Srai SK.** Molecular mechanisms involved in intestinal iron absorption. *World J Gastroenterol* 13: 4716–4724, 2007.

39. **Shepherd JD, Huganir RL.** The cell biology of synaptic plasticity: AMPA receptor trafficking. *Annu Rev Cell Dev Biol* 23: 613–643, 2007.

40. **Smith MD, Pannacciulli IM.** Absorption of inorganic iron from graded doses: its significance in relation to iron absorption tests and mucosal block theory. *Br J Haematol* 4: 428–434, 1958.

41. **Stewart WB, Yuile CL, Claiborne HA, Snowman RT, Whipple GH.** Radioiron absorption in anemic dogs; fluctuations in the mucosal block and evidence for a gradient of absorption in the gastrointestinal tract. *J Exp Med* 92: 375–382, 1950.

42. **Tabuchi M, Tanaka N, Nishida-Kitayama J, Ohno H, Kishi F.** Alternative splicing regulates the subcellular localization of divalent metal transporter 1 isoforms. *Mol Biol Cell* 13: 4371–4387, 2002.

43. **Tapia V, Arredondo M, Núñez MT.** Regulation of Fe absorption by cultured intestinal epithelia (Caco-2) cell monolayers with varied Fe status. *Am J Physiol Gastrointest Liver Physiol* 271: G443–G447, 1996.

44. **Thomas C, Oates PS.** Ferroportin/IREG-1/MTP-1/SLC40A1 modulates the uptake of iron at the apical membrane of enterocytes. *Gut* 53: 44–49, 2004.

45. **Tu GC, Cao QN, Zhou F, Israel Y.** Tetranucleotide GGGA motif in primary RNA transcripts. Novel target site for antisense design. *J Biol Chem* 273: 25125–25131, 1998.

46. **Van der AD, Marx JJ, Grobbee DE, Kamphuis MH, Georgiou NA, van Kats-Renaud JH, Breuer W, Cabantchik ZI, Roest M, Voorbij HA, van der Schouw YT.** Non-transferrin-bound iron and risk of coronary heart disease in postmenopausal women. *Circulation* 113: 1942–1949, 2006.

47. **Yeh KY, Yeh M, Watkins JA, Rodriguez-Paris J, Glass J.** Dietary iron induces rapid changes in rat intestinal divalent metal transporter expression. *Am J Physiol Gastrointest Liver Physiol* 279: G1070–G1079, 2000.

48. **Zurzolo C, Le Bivic A, Rodriguez-Boulan E.** Cell surface biotinylation techniques. In: *Cell Biology*, edited by Celis JE. San Diego, CA: Academic, 1994, p. 185–192.